IEEE Access
Multidisciplinary | Rapid Review | Open Access Journal

Received 20 November 2023, accepted 27 November 2023, date of publication 30 November 2023,
date of current version 8 December 2023.

Digital Object Identifier 10.1109/ACCESS.2023.3338239

RESEARCH ARTICLE

Fuzzy Control of Drilling Rig Winch Motor Based on SAWS-SSA Algorithm

YANWEI FENG[1] **AND LIXIN WEI**[2]
[1]Department of Mechanical Engineering, Tianshui Normal University, Tianshui 741000, China
[2]Department of Research and Development, Tianshui Electric Transmission Research Institute Group Company Ltd., Tianshui 741000, China

Corresponding author: Yanwei Feng (fyw0129@tsnu.edu.cn)

This work was supported in part by the Gansu Provincial Department of Education 2021 Industry Project under Grant 2021CYZC-42, and in part by the Tianshui Normal University 2021 Industry Project under Grant CYZC2021-02.

ABSTRACT This paper proposes an improved Sparrow Search Algorithm based on the self-avoiding random walk strategy as a fuzzy control method (SAWS-SSA) for rig winch motors in the complex oil rig electric control industry. The SAWS-SSA aims to accurately describe the system dynamics and improve the motor performance despite the large number of control-winch variables. During the startup of the three-phase asynchronous motor of the winch, the error value between the current feedback and thyristor trigger angle coupled with the periodic change rate was used as the input for the fuzzy control start. The fuzzy rules progressively reduce the components of the excitation current and iteratively calculate the difference between the input and feedback of the active power until the motor speed and torque are stabilized. To reduce the evaluation time of the optimization search, we optimized the heuristic affiliation function variables using an improved sparrow search algorithm equipped with a self-avoidance random walks strategy. Experimental verification confirms that SAWS-SSA outperforms other control algorithms in terms of the statistical error in the instantaneous dynamic response of the oil rig winch under a constant load and at different speeds.

INDEX TERMS Fuzzy control, self-avoiding random walks strategy, sparrow search algorithm, fuzzy rules.

I. INTRODUCTION

The control of oil industry drilling rigs is primarily motor-driven. An electronic control system is the primary equipment used to regulate the entire drilling-rig system. Currently, the market offers two types of systems: DC electric control and AC frequency conversion speed control. The frequency conversion speed control system has become a prevalent electrical transmission option owing to its precise and highly variable closed-loop control speed deviation performance, which is less than 3%, and its anti-jamming performance, which results in relative harmonics of the voltage output of less than 5% [1], [2], [3], [4]. The AC frequency-conversion electric control system of the drilling rig was operated using multiple diesel generator sets parallel to the grid or high-voltage grid power supply. The system outputs 600V 3φ50Hz AC power from the AC busbar, which is then converted into 810VDC power through the rectifier cabinet. The 810VDC is subsequently converted to 0-600VAC, frequency 0-150Hz continuously adjustable AC power by the inverter unit, which drives the motor to run. However, a nonlinear system dynamics model for three-phase asynchronous motors becomes difficult to describe when the torque and speed change frequencies are too fast [5]. Commonly used control methods in the petroleum industry include direct start control, pulse-width modulation (PWM) control, and vector control. Although several algorithms are available for adjusting motor speed, drilling pressure, and other parameters under specific loads, the stability, accuracy, and rapidity of the PID algorithm continue to dominate. Consequently, PID and its enhanced algorithms remain the best options for such adjustments. As on-site machines and equipment increase, a large and complex machine-electric-hydraulic cooperative control system emerges, resulting in a stronger correlation between control parameters and a higher degree of coupling between the multivariate input and output systems.

The associate editor coordinating the review of this manuscript and approving it for publication was Xiaojie Su.

Traditional parameter adjustment algorithms are no longer advantageous. Therefore, development of new control strategies and algorithms for highly complex systems is urgently required for practical engineering applications.

Traditional winch motors use vector frequency control with a core PID algorithm, resulting in a high control complexity and a relatively large cumulative error. This approach only allows for decoupling of the current excitation and torque components. Artificial intelligence iterative optimization parameter search algorithms have achieved positive results in speed regulation, drilling pressure stabilization, and harmonic filtering, including neural network algorithms [6], [7]. However, full-scale applications require a large amount of data for learning and training, particularly for data acquisition, preprocessing, and cleaning. Therefore, the reliability of the results must be verified for a significant amount of time [8], [9], [10]. The fuzzy control algorithm overcomes the drawbacks of the artificial intelligence algorithm when sudden changes occur in the real-time feedback signal of a rig winch. Moreover, owing to the variable-based decoupling principle (DVDP) and variable substitution principles (VSP), it is not necessary to establish mathematical models for this highly nonlinear system [11]. Nevertheless, the accuracy of the fuzzy control algorithm depends on the optimal affiliation function design and relevant fuzzy rules [12]. Usually, when parameter setting is conducted exclusively by human experience, it can cause unnecessary wastage of the equipment operation time.

Control optimization techniques are currently prevalent in industrial settings. Fuzzy control algorithms have been extensively studied from various perspectives to fine-tune the control parameters for efficient operation of the equipment. Lin and Dong [13] established less conservative stability conditions for T-S fuzzy systems with time-varying delays to verify the feasibility and superiority of these systems. Kuyu et al. [14] proposed a new algorithm that combines a backtracking search algorithm (BS) with a differential evolutionary algorithm (DE). The hybrid strategy ensures diversity of the initial population by applying diversity loss and stagnation detection mechanisms. Moreover, the adaptive modification strategy added to the variation operator of the new algorithm enables higher search capability. Kamarposhti et al. [15] proposed a whale intelligent algorithm to optimize the parameters of the fuzzy control algorithm, aiming to accurately track the maximum power of the system and obtain more effective power. Jamal et al. [16] proposed an adaptive fuzzy controller-based backtracking algorithm to drive a three-item asynchronous motor to obtain the minimum error of the affiliation function to improve the motor performance in terms of speed and torque variation. Guo et al. [17] selected a hyperbolic tangent function with a fuzzy boundary to replace the traditional tangent function and used an improved differential evolution algorithm to optimize the fuzzy rules to reduce the chattering and overshoot of the permanent magnet synchronous motor. Nsal and Aliskan [18] used a heuristic algorithm to optimize the output function of a fuzzy logic controller (FLC), combined with a genetic algorithm (GA) and gravitational search algorithm (GSA) to optimize the control performance of the FLC to obtain accurate changes in the PMSM speed control performance and electromagnetic torque. Albalawi et al. [19] proposed a torque control principle that can be directly applied to an asynchronous motor. The power converter was quickly mapped to the change in the torque. The ant colony search algorithm was used to optimize the fuzzy PID to improve the response time of the asynchronous motor and provide the best performance in terms of the speed and torque. Melin et al. [20] established a GT2 FLS model based on two-level categorical membership function fuzzy sets to obtain a set of Gaussian membership functions to improve the computational performance of fuzzy logic controllers. The optimal control has been extensively investigated by numerous researchers. However, this program has certain constraints and cannot satisfy the diverse working conditions of intricate control systems. To overcome this issue, self-avoiding random walk strategies are employed to avoid becoming trapped in local optima and to facilitate the search for a globally optimal solution.

The main contributions of this paper are as follows.

(1) To develop a unique fuzzy control model for a drilling rig winch motor and apply it to data collected from standard publicly accessible resources.

(2) To propose an improved sparrow search algorithm based on the self-avoiding random walk strategy as a fuzzy control method (SAWS-SSA) and compare the optimal speed control performance using various benchmark functions under constant load, regulating speed through the winch frequency converter with pulse-width modulation technology.

(3) To demonstrate the superiority of the proposed model over different machine-learning optimizations.

The remainder of this paper is organized as follows. In Section I, we discuss the related work of the various existing works on fuzzy control algorithms and intelligent optimization algorithms. Section II describes the proposed methodology using a brief mathematical model of self-avoiding random walk strategies and sparrow search algorithm. Section III presents the results obtained by performing experiments using the proposed model on the datasets collected from the CRWU datasets and compares them with existing models to demonstrate the performance superiority of the proposed SAWS-SSA model. Finally, Section IV concludes the study.

II. METHODOLOGY

The proposed method uses a drilling rig at depths below 5,000m, with a current suspension weight input of 30t (approximately 294kN). The winch motor had a power of approximately 800 kW and featured two braking resistors at 1200kW. To achieve optimal drilling speed, the system adjusts the feed-forward input of the inverter analog quantity by using the difference between the actual speed and the

recommended drilling speed, which should be between 0.8 and 1.2 times the recommended speed.

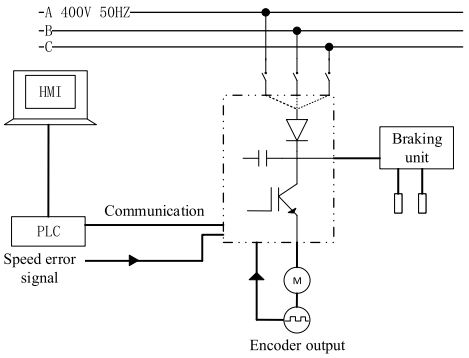

FIGURE 1. Block diagram of vector control.

A. SELF-AVOIDING RANDOM WALKS STRATEGY MODEL

The self-avoidance wandering strategy refers to a Markov Chain Model and random walks model based on lattice nodes [21], [22], [23]. This strategy assigns equal probabilities to all points in a multidimensional space that starting from a given point and not intersecting. If $\Psi \subset Z^d$ is a stochastic process and $\xi_1, \xi_2, \cdots, \xi_n$ satisfies the definition of an independently distributed random variable, then the practical application is dominated by the nearest-neighbor model and the extended model. The specific mathematical expressions for these models are shown in Equations (1) and (2).

$$\Psi = \left\{ x \in Z^d : ||x||_1 = 1 \right\} \tag{1}$$

$$\Psi = \left\{ x \in Z^d : 0 < ||x||_\infty \leq L \right\} \tag{2}$$

where L is a large integer. In a d dimensional dot grid, x begins at the initial position and uses the n-step vectors $S_n = (\xi_0, \xi_1, \cdots, \xi_n)$ to reach the endpoint of an n-step walk at that point. For any integer $i \in [1, n]$, there is $\xi_i - \xi_{i-1} \subset \psi$. The set of n-walks is defined by Equation (3).

$$S_n = \bigcup_{x \in Z^d} \xi_n(0, x) \tag{3}$$

The Z^d lattice space is defined by n-step walks $\xi \in S_n$ at x points. The integer s, t satisfies the condition $0 \leq s < t \leq n$, the mathematical model of the random path.

$$U_{s,t}(\xi) = \begin{cases} -1, & \xi(s) = \xi(t) \\ 0, & \xi(s) \neq \xi(t) \end{cases} \tag{4}$$

A random number between $\lambda \in [1, n]$ is added to each path vector as the Boltzmann weight factor of ξ, as shown in Equation (5).

$$\prod_{0 \leq s < t \leq n} (1 + \lambda U_{st}(\xi)) \tag{5}$$

Equation (6) defines the entire self-avoidance random walking process.

$$C_n^\lambda = \sum_{x \in Z^d} \sum_{\xi \in S_n} \prod_{0 \leq s < t \leq n} (1 + \lambda U_{st}(\xi)) \tag{6}$$

If $\lambda = 0$, all paths are assigned the same weight, which is called a simple random walk. If $\lambda = 1$, and if and only if each walk path accesses the grid point at most once, this method is called a self-avoiding walk. If $\lambda \in (0, 1)$, repeating the path through the grid node reduces the weight. However, this behavior is not avoided. This method is known as a weak self-avoidance walk.

According to the vector paradigm, C_n^λ satisfies the sub-vector multiplication rule shown in Equation (7).

$$\begin{aligned} C_{n+m}^\lambda \leq & \sum_{\xi \in S_{n+m}} \prod_{0 \leq s < t \leq n} \left(1 + \lambda U_{st}\right) \prod_{n \leq s' < t' \leq n+m} \left(1 + \lambda U_{s't'}\right) \\ & \times \sum_{\xi \in S_{n+m}} \prod_{0 \leq s < t \leq n} \left(1 + \lambda U_{st}\right) \\ & \times \prod_{n \leq s' < t' \leq n+m} \left(1 + \lambda U_{s't'}\right) \leq C_n^\lambda C_m^\lambda \end{aligned} \tag{7}$$

If there exists an $a_1, a_2, \cdots, a_n, \cdots, a_m \in R$ such that $a_{n+m} \leq a_n + a_m$ is satisfied for any m and n, then as shown in Equation (8).

$$\lim_{n \to \infty} \frac{a_n}{n} = \inf_{n \geq 1} \frac{a_n}{n} \in [-\infty, +\infty] \tag{8}$$

The existence of α_λ satisfying $\lim \log c_n^\lambda \Big/ n$ equal $\log \alpha_\lambda$ and $\log \alpha_\lambda \leq \log c_n^\lambda \Big/ n$, can be derived by combining Equations (7) and (8), as shown in Equation (9).

$$\alpha_\lambda = \lim_{n \to \infty} \left(c_n^\lambda\right)^{1/n}, c_n^\lambda \geq \alpha_\lambda^n \tag{9}$$

In the special case where $\lambda = 1, \alpha = \alpha_1$ is denoted by. The effective coordination number α is affected by both vector dimensions d and L in the extended model. However, the nearest neighbor model calculates the relationship described in Equation (9) by counting the positive coordinate directions and corresponding walking points.

$$d^n \leq c_n \leq 2d(d-1)^{n-1}, \quad d \leq \alpha \leq 2d - 1 \tag{10}$$

In Equation (10), when $d = 2$, the infimum is known, that is $\alpha \in [2.625622, 2.679193]$.

According to Hara scholars [24], asymptotic $1/d$ expansions exist for the connectivity constant of a self-avoiding tour across all orders by assuming that the residual term is of the same order of magnitude as the first omitted term in the inverse dimensional (also known as $1/d$ expansion) expansions, and proved that the effective number of collocations $\alpha(d)$ in the Z^d space in the nearest-neighbor model expands asymptotically on the $1/2d$ power when $d \to \infty$. In addition, there exists $a_i \in Z, i = -1, 0, 1, \ldots$, such that:

$$\alpha(d) \sim \sum_{i=-1}^{\infty} \frac{a_i}{(2d)^i} \tag{11}$$

The expression of variable $\alpha(d)$ at constant i equals $\alpha(d) = a_{-1}(2d) + a_0 + \cdots + a_{i-1}(2d)^{-(i-1)} + O(d^{-i})$, and the constant term $O(d^{-i})$ varies based on the value of i. $O(d^{-i})$ denotes the constraint term, which is less than negligible when the model is sufficiently complex and dimensional. Although it was expected that the asymptotic radius of convergence of Equation (11) would be zero, the convergence analysis indicated that the approach would be divergent.

In physical statistics, critical exponents describe the behavior near critical points. It has been experimentally proven that critical exponents have universal properties and are related solely to the spatial dimension of the system independent of its state. For the self-avoiding walk strategy, when $\lambda > 0$, the universal concept is extended to the application of a constant λ.

Assume the existence of a critical constant η for different d, such that all $\lambda \in (0, 1]$ satisfy both the nearest neighbor model and the extended model, as shown in Equation (12).

$$c_n^{\lambda} \sim A\xi_{\lambda}^{n} n^{\eta-1} \tag{12}$$

where A, ξ, η are standard numerical values. Let $\lim_{n\to\infty} f(n)/g(n) = \lim_{n\to\infty} c_n^{\lambda} \Big/ A\xi_{\lambda}^{n} n^{\eta-1} = 1$, be the projected value of the critical parameter M, as shown in Equation (13). The predicted critical value η is given by Equation (13).

$$\eta = \begin{cases} 1 & d = 1 \\ 43/32 & d = 2 \\ 1.16\ldots & d = 3 \\ 1 & d = 4 \\ 1 & d \geq 5 \end{cases} \tag{13}$$

The self-avoiding walk strategy focuses on the core problem of evaluating the best position using efficient search abilities, judging convergence under different dimensions, and obtaining the global optimal position.

B. SPARROW SEARCH ALGORITHM

The sparrow search algorithm is known for its strong optimization abilities, simple structure, minimal control parameters, and fast convergence speed compared to traditional optimization search algorithms [25], [26], [27], [28]. The sparrow search algorithm mainly simulates the sparrow foraging process called the explorer-follower process, enhances the early warning detection mechanism, and identifies the sparrows that discover areas with better food sources, providing those areas and following their directions. The remaining individuals acted as followers, and randomly, 10% to 20% of the individuals were selected for investigation and early warning sparrows. There is also competition for food among sparrows within the population. In situations of danger, foraging behavior is abandoned.

We assume that the number of sparrow populations is expressed in the matrix form in Equation (14).

$$X = \begin{bmatrix} x_1^1 & x_1^2 & \cdots & x_1^d \\ x_2^1 & x_2^2 & \cdots & x_2^d \\ \cdots & \cdots & \ddots & \cdots \\ x_n^1 & x_n^2 & \cdots & x_n^d \end{bmatrix} \tag{14}$$

where d represents the dimension of the variable to be optimized, n represents the number of sparrows, and the fitness value f of each sparrow is expressed by Equation (15).

$$F_x = \begin{bmatrix} f\left[x_1^1 \; x_1^2 \; \cdots \; x_1^d\right] \\ f\left[x_2^1 \; x_2^2 \; \cdots \; x_2^d\right] \\ \cdots \\ f\left[x_n^1 \; x_n^2 \; \cdots \; x_n^d\right] \end{bmatrix} \tag{15}$$

Prior to establishing a mathematical model, it was necessary to establish certain rules. Typically, the explorer has a considerable energy reserve and assumes the responsibility of searching for areas with abundant food as well as providing foraging areas and directions to followers. During the model establishment, the energy reserve level of an individual sparrow depends on its fitness value. If the alarm value exceeds the safety threshold, the leader directs followers to forage in other areas. The foraging position deteriorates with decreasing energy reserves of followers. Within the SSA, an explorer with better fitness prioritizes obtaining food. The explorer's position is updated during each iteration according to Equation (16).

$$X_{i,d}^{t+1} = \begin{cases} X_{i,d}^{t} \cdot \exp\left(\dfrac{-i}{\alpha \cdot iter_{\max}}\right) & R_2 < ST \\ X_{i,d}^{t} + Q & R_2 \geq ST \end{cases} \tag{16}$$

where $X_{i,d}^{t}$ denotes the d dimensional position of the i individual in the generation of population t generation, $\alpha \in (0, 1]$ denotes a uniform random number in the range of 0 to 1, $iter_{\max}$ denotes the maximum number of iterations, Q denotes a random number obeying a standard normal distribution, R_2 denotes the warning value taking the value of [0, 1], and ST denotes the safety value taking the value of [0.5, 1]. When $R_2 < ST$, the environment was safe, the foraging area expanded, and the value gradually became uniform as the number of iterations increased. When $R_2 \geq ST$, it means that an explorer has already found the danger and turns to other areas to forage; that is the explorer is randomly moved to the current position according to the normal distribution, and its position converges to the optimal position.

The location update formula for the follower is presented in Equation (17).

$$X_{i,d}^{t+1} = \begin{cases} Q \cdot \exp\left(\dfrac{X_{worst}^{t} - X_{i,d}^{t}}{i^2}\right) & i > n/2 \\ X_P^{t+1} + \left|X_{i,d}^{t} - X_P^{t+1}\right| \cdot A^{+} \cdot L & i \leq n/2 \end{cases} \tag{17}$$

where X_P represents the optimal explorer position, and X_{worst} represents the global worst position. If A is a $1 \times d$ matrix,

where the value of each element is $Rand\{1, 1\}$, then $A^+ = A^T(AA^T)^{-1}$. When $i > n/2$, its value is obtained by multiplying a standard normally distributed random number with an exponential function. The i follower with lower fitness needs to go to other regions to obtain more energy reserves due to food shortages. When $i \leq n/2$, the difference between the current and optimal values in the same dimension is small.

Individuals were randomly selected for investigation and early warning, and their location updates are shown in Equation (18).

$$X_{i,d}^{t+1} = \begin{cases} X_{best}^t + \beta \cdot \left| X_{i,d}^t - X_{best}^t \right| & f_i > f_g \\ X_{i,d}^t + K \cdot \left(\dfrac{\left| X_{i,d}^t - X_{worst}^t \right|}{(f_i - f_w) + \varepsilon} \right) & f_i = f_g \end{cases} \tag{18}$$

where X_{best} represents the current global optimal position and β is a step control parameter that follows a normal distribution. $K \in [-1, 1]$ is a random number. f_i represents the current individual fitness value, f_g and f_w represent the global optimal fitness value and the worst fitness value, respectively. ε has an extremely small numerical value that prevents the denominator from being zero.

The sparrow search algorithm exhibits high search accuracy and robustness in the multi-objective optimization process. However, the convergence speed of the algorithm for the entire objective function is affected when the parameters are set differently, which makes it prone to local optimal solutions. This can lead to uncertainty in the results of large search spaces. Hence, it is necessary to develop an approach to improve the convergence and optimal solution ability of sparrow search algorithms in various search spaces.

C. FUZZY CONTROL BASED ON SAWS-SSA ALGORITHM

The swarm intelligence optimization algorithm SSA is based on sparrow foraging and anti-hunting. The SAWS strategy was employed to increase the SSA's global optimization search capability and enhance its optimal path. The initial population positions have different search capabilities, according to the basic principles of SSA. The SAWS-SSA global explorer was tentatively determined by evaluating the average values of the best paths. The explorer's flight step and convergence ability are used to attract the remaining followers to achieve SAWS-SSA global optimal solution and the best path. Equation (19) shows the random attractor equation for the step explorer.

$$p_{x^d}^{iter} = \frac{k_{x^d}^{iter} \cdot Best(P_{x^d}^{iter}) + m_{x^d}^{iter} \cdot (s_{x^d}^{iter}/M)}{n_{x^d}^{iter} \cdot SF} \tag{19}$$

where the parameters used include $x = 1, 2, \ldots, N$ for the number of populations, $d = 1, 2, \ldots, D$ for the problem dimension, $iter = 1, 2, \ldots, T$ for the maximum number of iterations, k, m, n for the number of uniform distributions of $rand(0, 1)$, respectively, $Best(p_{x^d}^{iter})$ for the optimal explorers under different populations, $s_{x^d}^{iter}$ for the optimal path distance, M for the optimal number of paths under different populations, and SF for the scaling factor. The value of SF is usually approximately 12, and should not be too large or too small.

It is assumed that the explorers of each population exhibit self-walking behavior. The double exponential distribution can reflect the exponential distribution of two different positions and follows the Laplace distribution, making it appropriate for describing sparrow search behavior. Equation (20) shows that the probability density function is expressed as $F_P(p)$.

$$F_P\left(p_{x^d}^{iter+1}\right) = \frac{1}{(L_{x^d}^{iter})^{1/2}} \exp\left(-\frac{|Best(P_{x^d}^{iter}) - p_{x^d}^{iter}|}{L_{x^d}^{iter}}\right) \tag{20}$$

where $L_{x^d}^{iter}$ represents the binomial distribution and $F_P(p)$ changes with iteration. The attractor equation following $iter + 1$ is using the Monte-Carlo method, as shown in Equation (21).

$$P_{x^d}^{iter+1} = p_{x^d}^{iter} \pm \frac{1}{2} L_{x^d}^{iter} \ln(1/\delta_{x^d}) \tag{21}$$

where variable δ_{x^d} represents a uniformly distributed random number between 0 and 1. The convergence rate of the SAWS-SSA is controlled by enhancing the attribute features using the contraction-expansion coefficient β. Equation (22) expresses β.

$$\beta = \beta_{\min} + (iter_{\max} - iter) \cdot \frac{\beta_{\max} - \beta_{\min}}{iter_{\max}} \tag{22}$$

where $iter_{\max} = T$ denotes the maximum number of iterations, $iter$ denotes the current number of iterations, $\beta_{\min}$ denotes the initial value of the contraction-expansion coefficient, and the general value is less than 0.6. $\beta_{\max}$ represents the end value of the contraction-expansion coefficient, which is greater than 0.8. β is linearly reduced during the entire iteration process. Combined with Equations (19)-(22), the expression of updated position of the sparrow explorer is shown in Equation (23).

$$P_{x^d}^{iter+1} = p_{x^d}^{iter} \pm \beta \left| \frac{1}{M} \sum s_{x^d}^{iter} - P_{x^d}^{iter} \right| \ln(1/\delta_{x^d}) \tag{23}$$

SAWS-SSA can overcome the limitations of SSA and enhances the accuracy and search capability by using an exponential distribution function to globally converge the search for new explorer locations and by evaluating the criterion.

Fuzzy control is a type of rule-based nonlinear control designed using heuristic knowledge and linguistic decision rules. Fuzzy control algorithms were used to control the inverter voltage and frequency, which resulted in an improved ramp-up time for the controlled motor and enhanced the robustness of the system. Fuzzy speed control includes several parameters, such as the affiliation function, rule base, and fuzzy rules. Optimizing these parameter values improves the efficiency of fuzzy speed control. Triangle and trapezoidal affiliation functions were utilized to express the speed

error (e) and error variation (de) of the three-phase asynchronous motor, as presented in Equations (24) and (25).

$$\varepsilon_e(e) = \begin{cases} \dfrac{e - A_0}{A_1 - A_0} & A_0 \le e \le A_1 \\ \dfrac{A_2 - e}{A_2 - A_1} & A_1 \le e \le A_2 \end{cases} \tag{24}$$

$$\varepsilon_{de}(de) = \begin{cases} \dfrac{e - B_0}{B_1 - B_0} & B_0 \le de \le B_1 \\ \dfrac{A_2 - e}{A_2 - A_1} & B_1 \le de \le B_2 \end{cases} \tag{25}$$

where the shape of the curve is determined by the parameters $A_0, A_1, A_2, B_0, B_1, B_2$. The Mamdani Fuzzy Rule method employs an if-then language description to establish rules that determine the fuzzy relationship between the input (e, de) and output speed (ω_s) because of its simplicity and practicality. Evaluating the minimum value of the objective function yields an optimal membership function. Equation (26) defines the objective function.

$$OF = \min\left(\frac{1}{z}\sum_{m=1}^{M}\left|\omega' - \omega\right|\right) \tag{26}$$

where z is the number of sample spaces, ω' is the reference rotational speed, and ω is the actual rotational speed.

The SAWS-SSA addresses the deficiencies of the SSA, which is prone to slow convergence, local optima, and sensitivity to the output parameters. This algorithm employs a mathematical model to enhance the global search capability using a self-avoiding exponential random walk strategy with a constant step size to avoid the uncertainty and perturbations generated by the search path and to increase the speed of the optimization search until iteration completion. The SAWS-SSA was designed, and its step response signals were tested with the same population size (50) and number of iterations (300). Furthermore, the performance of this algorithm was compared with those of the ACO, GSA, PSO, and SAWS-SSA algorithms to establish their effectiveness and consistency.

III. EXPERIMENT AND ANALYSIS

A. DATASETS AND EXPERIMENT SETTING

The hardware used in the experiment consisted of Windows 10 Professional, Intel(R) Core (TM) i7 2.3 GHz processor, and MATLAB 2018b/Simulink software. The SAWS-SSA algorithm proposed in this study avoids utilizing the traditional exhaustive heuristic method to obtain the affiliation function values. Instead, ten sets of baseline functions were used to examine the precision and adaptability of the algorithm on the CRWU datasets presented in Table 1. These datasets include the Drive End, Fan End, and Baseline measurements of the motor at 12k/48k sampling frequency. To enhance the generalization ability of the datasets, the data were reorganized using shuffle() and batch() functions in Python. Because the datasets comprise normal and faulty samples, the effectiveness of the SAWS-SSA was verified by extracting motor speed parameters under normal samples based on various motor loads.

TABLE 1. Benchmark function description.

NO.	Function	Lower_bound	Upper_bound
F1	Ackley function	-32.78	32.78
F2	Alpine function	-15	15
F3	BartelsConn function	-100	100
F4	Beale function	-10	10
F5	Camel function	-2	2
F6	Hosaki function	0	6
F7	Jennrich function	-1	0.35
F8	Keane function	0	10
F9	Leon function	-1.2	1.2
F10	Chichinadze function	-10	10

B. RESULTS AND DISCUSSIONS

The motor performance is influenced by several factors, such as load, interference, and control mode, which result in nonlinear trends in data such as speed and torque. To demonstrate the effectiveness of the SAWS-SSA, we evaluated its validity on the ten nonlinear benchmark functions mentioned earlier. We obtained the global optimal solution for these functions. Figure 2 displays a three-dimensional graphical representation of the benchmark functions. F1 represents a continuously non-convex function with numerous local minima. However, it possesses a single global minimum with a fixed value of zero. F2 is a classical multimodal minimization test function. When tending to infinity in the domain of definition, this function produces a large number of differentiable local extrema along the direction of the independent variables, which are difficult to optimize. F3 is a continuous and unscalable function with a function value of 1. F4 is a nonlinear function with multiple local minima as well as globally. F5 is a continuous function with multiple local minima, two of which are global minima. F6 is a function that is continuously differentiable and non-integrable. F7 is a concave-convex combination of functions. F8 is a function that is continuous, with multiple minima. F9 represents a non-convex function with a global minimum of 0. F10 is a function that is continuously differentiable and integrable with a global minimum of -43.315.

To further verify the superior performance of SAWS-SSA under various benchmark functions, the convergence of the Ant Colony Search Algorithm (ACO), Gravitational Search Algorithm (GSA), and Particle Swarm Optimization Algorithm (PSO) was compared. Figure 3 illustrates the convergence trend of the F1-F4 optimization iteration number 300. ACOF1 indicates that the ACO fuzzy algorithm converges after 25 iterations of the F1 function, resulting in an optimal fitness value of 0.1218. In contrast, the GSA fuzzy

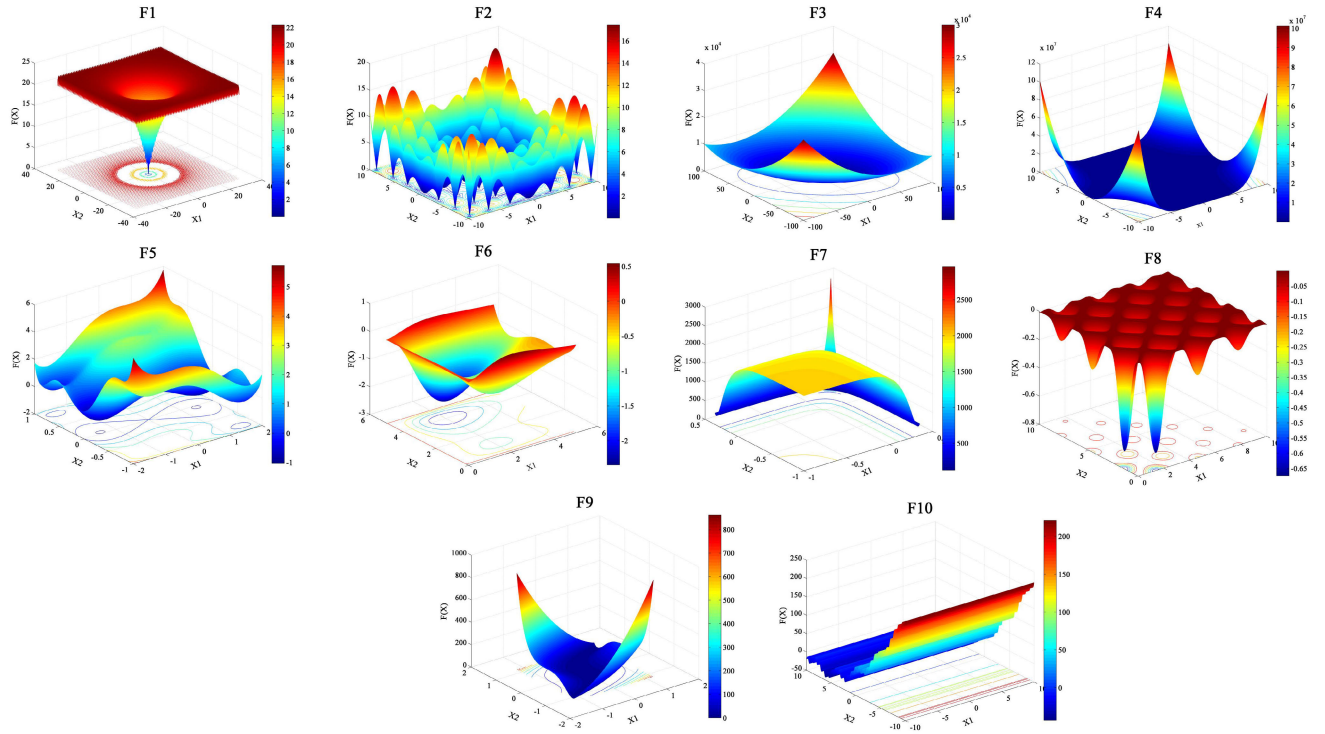

FIGURE 2. Benchmarking functions.

algorithm required 161 iterations of the F1 function, resulting in an optimal fitness value of 0.0183. Meanwhile, the PSO fuzzy algorithm required 183 iterations of the F1 function, resulting in an optimal fitness value of 0.0183. Finally, the SAWS-SSA fuzzy algorithm required only 16 iterations of the F1 function, resulting in convergence with an optimal fitness value of 0.0171. A thorough analysis conducted on the ACO fuzzy algorithm revealed that although it had a similar number of iterations to that of the SAWS-SS fuzzy algorithm, its convergence speed was significantly worse than that of the SAWS-SSA fuzzy algorithm. The SAWS-SSA outperformed the other algorithms in terms of the F1 function. Comparing the convergence trend graph of the F2 function, it is apparent that the SAWS-SSA has a faster convergence speed and smaller optimal fitness value than the ACO, GSA, and PSO fuzzy algorithms. Specifically, while the number of iterations for all algorithms was similar (132, 164, 182, and 182, respectively), the SAWS-SSA outperformed the others in terms of convergence speed and fitness value according to the graph. The PSO fuzzy algorithm displays superior convergence speed, a higher number of iterations (25), and an optimal fitness value (0.0149) compared to the ACO, GSA, and the SAWS-SSA fuzzy algorithms in the F3 function. In addition, SAWS-SSA achieved optimal performance in the F4 function.

Figure 2 illustrates that the benchmark functions are multimodal and that functions F5-F10 contain multiple minima. As the function dimensions increased, the minima exhibited nonlinear growth, emphasizing the importance of the algorithm's ability to escape local optima. Table 2 displays the results obtained over 300 iterations for functions F5 through F10, measuring four aspects: average of best fitness, median of best fitness, average of mean fitness, and overall best fitness.

Table 2 shows that the SAWS-SSA algorithm has significantly better performance in the F5, F9, and F10 datasets. Meanwhile, the GSA algorithm has the best performance in the F6 datasets. The results of the SAWS-SSA, ACO, and PSO optimization searches in the F7 and F8 data are similar. However, the SAWS-SSA algorithm performs relatively better.

During field operations, various parameters are adjusted based on factors such as drill bit size, drilling tools, and geology. To obtain results that closely resembled those in the field, the system was simulated experimentally. The sampling time was set to 500ms ($t = 500$ms) with a maximum of 200 iterations ($iter_{\max} = 200$) and a population size of 50 ($n = 50$). A warning value of 0.5 ($R_2 = 0.5$) and a safety value of 0.8 ($ST = 0.8$) are used, along with a bandwidth of 0.7 ($\lambda = 0.7$), compensation coefficient of 0.6 ($b_0 = 0.6$), and an error coefficient of 0.02 ($k_0 = 0.02$). To simulate the interference situation in the field more accurately, superposition of white noise was used as the actual signal input.

The SAWS-SSA algorithm reduces the current component and calculates the input and feedback difference of the active power iteratively until the motor speed achieves stability. Figure 1 depicts a block diagram of the three-phase motor vector control.

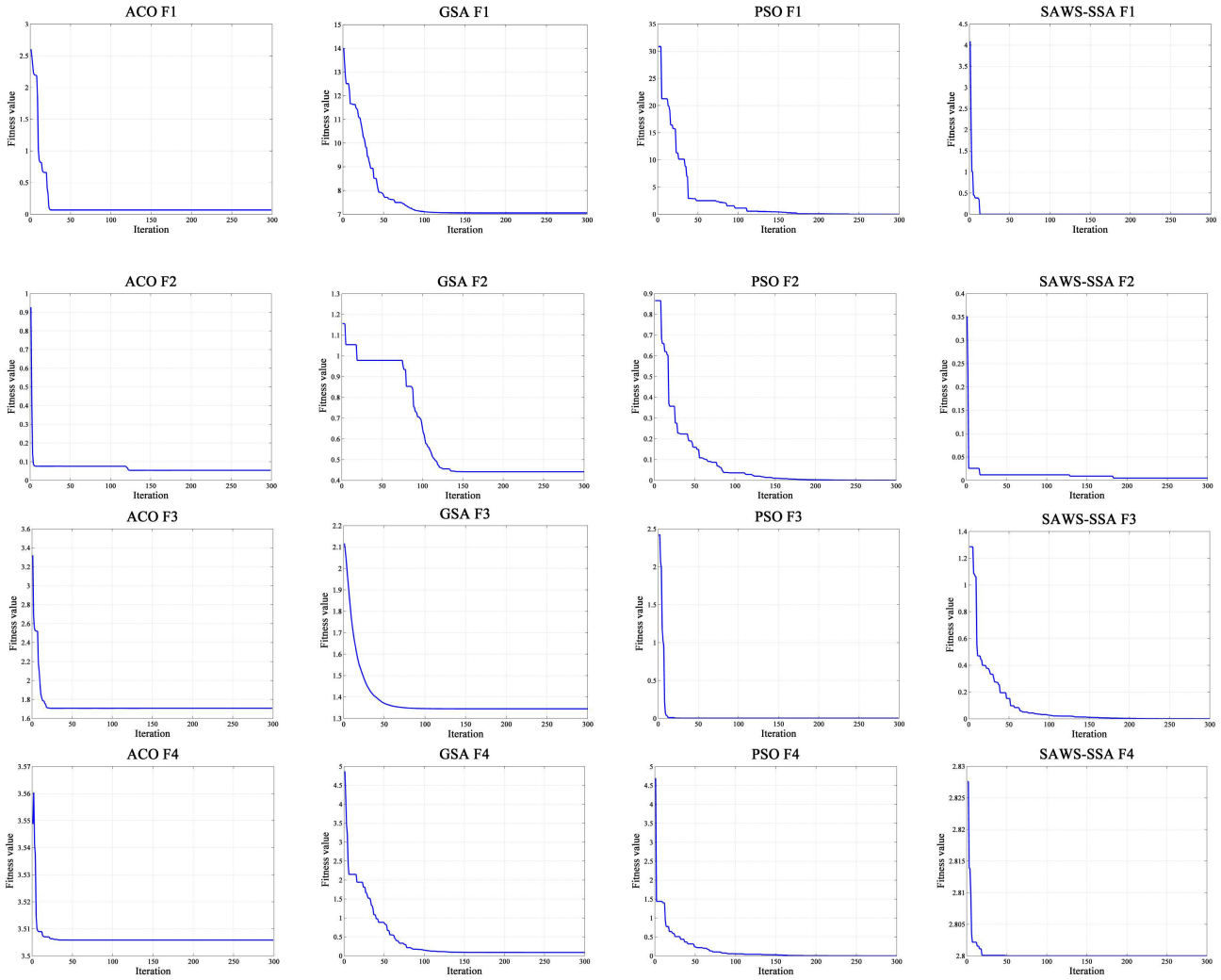

FIGURE 3. Function convergence characteristics under algorithm.

Although the performance of the SAWS-SSA has been verified, it is uncertain whether the SAWS-SSA algorithm is effective after the fusion of the fuzzy control algorithm. Therefore, in the step response, we compared the accuracy and effectiveness of the SAWS-SSA algorithm with the fuzzy control-based ACO, GSA, and PSO algorithms.

Figure 4 shows that the SAWS-SSA algorithm has the best convergence characteristics. Figure 5 shows the maximum boundary error variation values of the membership function, where Ne3, Ne2, and Ne1 describe the size of the boundary error when the degree of ambiguity is negative, and Pe1, Pe2, and Pe3 describe the size of the boundary error when the degree of ambiguity is positive. Figure 6 depicts the variation in the error of the output value of the membership function. Nde3, Nde2, and Nde1 refer to the output error size when the degree of fuzziness is negative, whereas Pde1, Pde2, and Pde3 refer to the output error size when the degree of fuzziness is positive. Figure 7 illustrates the degree of fuzziness of the membership function. Specifically, the degree of fuzziness of NB is significantly negative, NM is moderately negative, and NS is slightly negative. The degree of fuzziness of Z is neutral (0), whereas that of PS is slightly positive, PM is moderately positive, and PB is significantly positive. Figures 5-7 show the membership function error and error variation range between $[-3, 3]$ and the output range of $[-6, 6]$. Moreover, we used the SAWS-SSA to determine the best membership function value for three-phase asynchronous motor slip speeds.

The adaptability of the SAWS-SSA algorithm under a constant load and changing speed was evaluated using step response. First, the speed was increased from 1/4 (370 rpm/min) to half speed (750 rpm/min) and then further increased to full speed (1500 rpm/min) after 1s. The mean absolute error (MAE), root-mean-square error (RMSE), and standard deviation (SD) are 2.374%, 16.543%, and 16.121%, respectively. Compared to other algorithms, SAWS-SSA exhibits a lower mean absolute error (MAE), root-mean-square error (RMSE), and stan-

TABLE 2. The results after 300 iterations of F5 - F10.

NO.	Function	Attribute	ACO	GSA	PSO	SAWS-SSA
F5	Camel	Average of best fitness	0.511	2.000	0.000	0.000
		Median of best fitness	0.214	4.12×10^{-5}	0.000	0.000
		Average of mean fitness	0.222	1.739	3.682	0.711
		Overall best fitness	0.016	7.25×10^{-6}	0.000	0.000
F6	Hosaki	Average of best fitness	5.212	1.032	4.689	3.288
		Median of best fitness	5.055	1.032	2.871	3.322
		Average of mean fitness	5.212	0.947	4.689	3.288
		Overall best fitness	5.322	1.031	6.064	3.322
F7	Jennrich	Average of best fitness	2.44×10^{-3}	1.23×10^{-3}	4.33×10^{-3}	2.04×10^{-4}
		Median of best fitness	1.24×10^{-3}	5.01×10^{-4}	3.53×10^{-4}	1.99×10^{-4}
		Average of mean fitness	2.08×10^{-4}	1.97×10^{-3}	4.34×10^{-4}	2.05×10^{-4}
		Overall best fitness	6.47×10^{-4}	3.07×10^{-4}	3.07×10^{-4}	1.88×10^{-4}
F8	Keane	Average of best fitness	5.776	6.994	6.036	5.232
		Median of best fitness	5.893	6.827	6.533	5.113
		Average of mean fitness	5.867	6.992	6.101	4.898
		Overall best fitness	5.630	6.646	4.588	5.070
F9	Leon	Average of best fitness	1.90×10^{-5}	1.57×10^{-5}	1.20×10^{-5}	1.06×10^{-5}
		Median of best fitness	1.89×10^{-5}	1.59×10^{-5}	1.22×10^{-5}	1.06×10^{-5}
		Average of mean fitness	1.90×10^{-5}	1.61×10^{-5}	1.18×10^{-5}	1.04×10^{-5}
		Overall best fitness	1.83×10^{-5}	1.50×10^{-5}	1.24×10^{-5}	1.11×10^{-5}
F10	Chichinadz	Average of best fitness	6.991	6.166	9.911	5.067
		Median of best fitness	6.828	8.539	1.748	5.656
		Average of mean fitness	6.991	6.103	9.941	6.354
		Overall best fitness	6.644	4.584	1.028	5.486

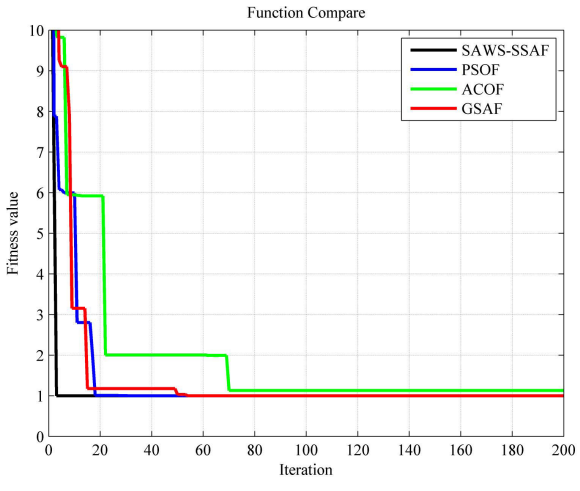

FIGURE 4. Convergence properties of different algorithms.

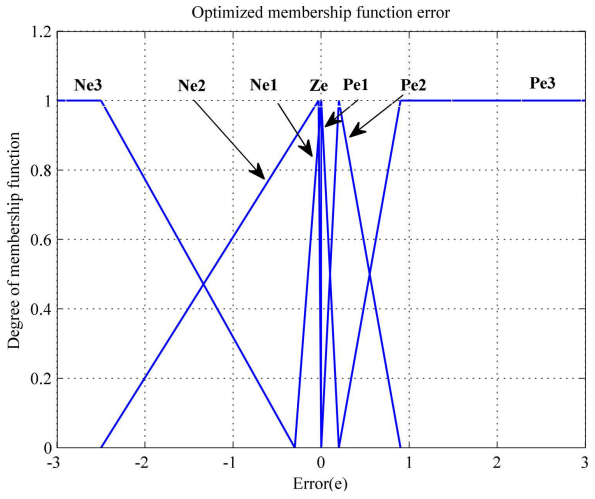

FIGURE 5. The error of membership function.

dard deviation (SD) with minimal overshooting when the speed suddenly changes. Please refer to Figure 8 for a step response.

In summary, the SAWS-SSA algorithm exhibits a steady-state error below 0.1%, with fast convergence and high control precision, which confirms its effectiveness.

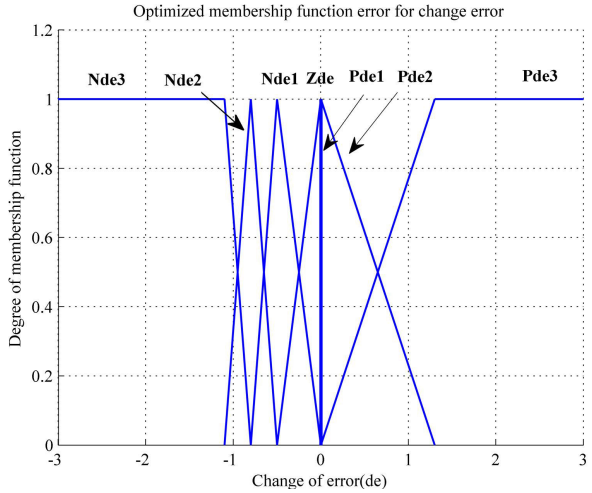

FIGURE 6. The error change of membership function.

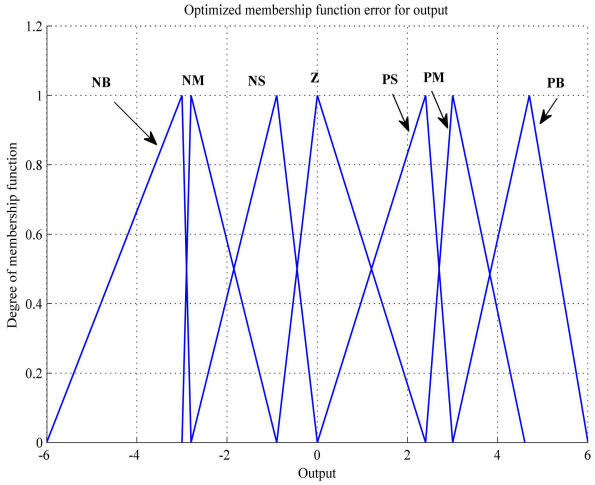

FIGURE 7. The output of membership function.

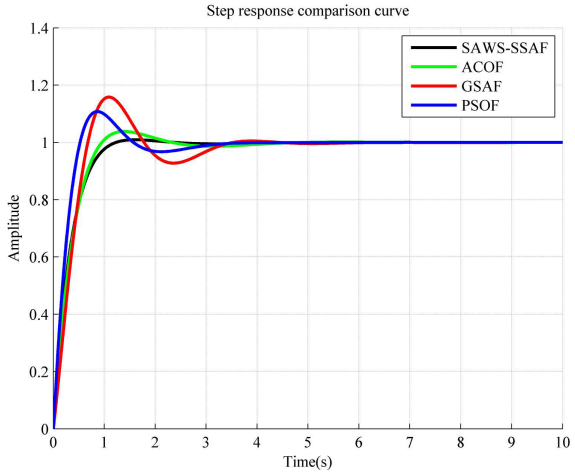

FIGURE 8. Comparison curve of step response.

The design concept is elaborated on while integrating other real signals.

IV. CONCLUSION

The process of controlling the winch in the electronic control system of the oil drilling rig is complex, and accurately describing the system dynamics and improving the motor performance is difficult. This difficulty results in inaccurate and ineffective motor controls. We used the SAWS-SSA algorithm, which is based on the self-avoiding random walk strategy and improved sparrow search method, to iteratively calculate the input and feedback difference of the active power. This stabilized and accurately controlled the speed and torque of the motor. The simulation results demonstrated that the algorithm designed in this study can improve the control speed and quickly bring the system parameters to the best state. This confirms the superiority and effectiveness of the algorithm and its potential application in the electric control systems of drilling rigs.

REFERENCES

[1] C. Cong, "Research on automatic control method of drilling speed and torque in oil drilling," *Autom. Instrum.*, vol. 246, no. 4, pp. 91–94, Jun. 2020.

[2] H. Wang, H. Huang, W. Bi, G. Ji, B. Zhou, and L. Zhuo, "Deep and ultra-deep oil and gas well drilling technologies: Progress and prospect," *Natural Gas Ind. B*, vol. 9, no. 2, pp. 141–157, Apr. 2022.

[3] G. Li, X. Song, S. Tian, and Z. Zhu, "Intelligent drilling and completion: A review," *Engineering*, vol. 18, pp. 33–48, Nov. 2022.

[4] A. Nobahar, K. B. Arıkan, M. E. Özbek, and B. Naseri, "Performance assessment of tripping and drilling operations controllers on an experimental drilling rig prototype," *Geoenergy Sci. Eng.*, vol. 226, Jul. 2023, Art. no. 211758.

[5] X. Hong, C. Zhu, S. An, and Y. Zhao, "Simulation analysis of transient output characteristics of inverter with asynchronous motor load based on second-order filtering link," *Sustain. Energy Technol. Assessments*, vol. 49, Feb. 2022, Art. no. 101725.

[6] G. Tan and Z. Wang, "Reachable set estimation of delayed Markovian jump neural networks based on an improved reciprocally convex inequality," *IEEE Trans. Neural Netw. Learn. Syst.*, vol. 33, no. 6, pp. 2737–2742, Jun. 2022.

[7] J. Hu, G. Tan, and L. Liu, "A new result on H_∞ state estimation for delayed neural networks based on an extended reciprocally convex inequality," *IEEE Trans. Circuits Syst. II, Exp. Briefs*, pp. 1–5, 2023, doi: 10.1109/TCSII.2023.3323834.

[8] L. Wang, Y. Yao, X. Luo, C. D. Adenutsi, G. Zhao, and F. Lai, "A critical review on intelligent optimization algorithms and surrogate models for conventional and unconventional reservoir production optimization," *Fuel*, vol. 350, Oct. 2023, Art. no. 128826.

[9] C. Shi and X. Feng, "Optimization of carbon emission peak path based on multisensor information fusion and integrated intelligent algorithm," *Energy Rep.*, vol. 8, pp. 11174–11180, Nov. 2022.

[10] X. Wang, X. Li, and S. Li, "Point and interval forecasting system for crude oil price based on complete ensemble extreme-point symmetric mode decomposition with adaptive noise and intelligent optimization algorithm," *Appl. Energy*, vol. 328, Dec. 2022, Art. no. 120194.

[11] Y. Tian and Z. Wang, "Finite-time extended dissipative filtering for singular T–S fuzzy systems with nonhomogeneous Markov jumps," *IEEE Trans. Cybern.*, vol. 52, no. 6, pp. 4574–4584, Jun. 2022.

[12] D. Bao, X. Liang, S. S. Ge, Z. Hao, and B. Hou, "A framework of adaptive fuzzy control and optimization for nonlinear systems with output constraints," *Inf. Sci.*, vol. 616, no. 10, pp. 411–426, Nov. 2022.

[13] H. Lin and J. Dong, "Stability analysis of T–S fuzzy systems with time-varying delay via parameter-dependent reciprocally convex inequality," *Int. J. Syst. Sci.*, vol. 54, no. 6, pp. 1289–1298, Feb. 2023.

[14] Y. Ç. Kuyu, E. Onieva, and P. Lopez-Garcia, "A hybrid optimizer based on backtracking search and differential evolution for continuous optimization," *J. Experim. Theor. Artif. Intell.*, vol. 34, no. 3, pp. 355–385, May 2022.

[15] M. A. Kamarposhti, H. Shokouhandeh, I. Colak, and K. Eguchi, "Optimization of adaptive fuzzy controller for maximum power point tracking using whale algorithm," *Comput., Mater. Continua*, vol. 73, no. 3, pp. 5041–5061, 2022.
[16] J. A. Ali, M. A. Hannan, A. Mohamed, and M. G. M. Abdolrasol, "Fuzzy logic speed controller optimization approach for induction motor drive using backtracking search algorithm," *Measurement*, vol. 78, pp. 49–62, Jan. 2016.
[17] L. Guo, X. Zhang, C. Zheng, P. Zhang, and X. Wu, "A new fuzzy sliding mode control method for permanent magnet synchronous motor servo system based on optimization of fuzzy rules," *IEEJ Trans. Electr. Electron. Eng.*, vol. 17, no. 12, pp. 1748–1754, Aug. 2022.
[18] S. Ünsal and I. Aliskan, "Investigation of performance of fuzzy logic controllers optimized with the hybrid genetic-gravitational search algorithm for PMSM speed control," *Automatika*, vol. 63, no. 2, pp. 313–327, Apr. 2022.
[19] H. Albalawi, S. A. Zaid, M. E. El-Shimy, and A. M. Kassem, "Ant colony optimized controller for fast direct torque control of induction motor," *Sustainability*, vol. 15, no. 4, p. 3740, Feb. 2023.
[20] P. Melin, E. Ontiveros-Robles, C. I. Gonzalez, J. R. Castro, and O. Castillo, "An approach for parameterized shadowed type-2 fuzzy membership functions applied in control applications," *Soft Comput.*, vol. 23, no. 11, pp. 3887–3901, Jun. 2019.
[21] P. Preeti and K. Deep, "A random walk grey wolf optimizer based on dispersion factor for feature selection on chronic disease prediction," *Exp. Syst. Appl.*, vol. 206, Nov. 2022, Art. no. 117864.
[22] C. J. Bradly and A. L. Owczarek, "Polymer collapse of a self-avoiding trail model on a two-dimensional inhomogeneous lattice," *Phys. A, Stat. Mech. Appl.*, vol. 604, Oct. 2022, Art. no. 127688.
[23] J. R. Britnell and M. Wildon, "Involutive random walks on total orders and the anti-diagonal eigenvalue property," *Linear Algebra Appl.*, vol. 641, pp. 1–47, May 2022.
[24] T. Hara and G. Slade, "The self-avoiding-walk and percolation critical points in high dimensions," *Combinatorics Probab. Comput.*, vol. 4, no. 3, pp. 197–215, Sep. 1995.
[25] J. Li, J. Chen, and J. Shi, "Evaluation of new sparrow search algorithms with sequential fusion of improvement strategies," *Comput. Ind. Eng.*, vol. 182, Aug. 2023, Art. no. 109425.
[26] R. Wu, H. Huang, J. Wei, C. Ma, Y. Zhu, Y. Chen, and Q. Fan, "An improved sparrow search algorithm based on quantum computations and multi-strategy enhancement," *Exp. Syst. Appl.*, vol. 215, Apr. 2023, Art. no. 119421.
[27] T. Arulkumar and N. Chandrasekaran, "Development of improved sparrow search-based PI controller for power quality enhancement using UPQC integrated with medical devices," *Eng. Appl. Artif. Intell.*, vol. 116, no. 12, pp. 444–455, Sep. 2022.
[28] Z. Xing, C. Yi, J. Lin, and Q. Zhou, "Multi-component fault diagnosis of wheelset-bearing using shift-invariant impulsive dictionary matching pursuit and sparrow search algorithm," *Measurement*, vol. 178, Jun. 2021, Art. no. 109375.

YANWEI FENG received the B.S. degree in mechanical manufacturing and automation from the Lanzhou University of Technology, Lanzhou, China, in 1995.

From 1995 to 2020, he was a Chief Engineer with Lanzhou LS Petroleum Equipment Engineering Company Ltd. Since 2020, he has been a Professor with the Mechanical and Automotive Engineering Department. He is currently a Professor with the Department of Mechanical and Automotive Engineering, Tianshui Normal University, China. His current research interests include mechanical system design for oil drilling equipment, oil and gas drilling equipment inspection, and troubleshooting technology.

Dr. Feng is a China Petroleum and Petrochemical Equipment Industry Association of Experts. He won the First Prize for Gansu Provincial Scientific and Technological Progress.

LIXIN WEI received the B.S. degree in computer science and technology from Ludong University, Yantai, China, in 2016, and the M.S. degree in computer science and technology from Lanzhou Jiaotong University, Lanzhou, China, in 2020. He is currently an Intermediate Engineer with Tianshui Electric Transmission Research Institute Group Company Ltd. His current research interest includes intelligent control algorithm design for oil drilling rigs.